

# Dynamic Response of Pile in Saturated Porous Medium Considering Radial Heterogeneity by Pile Driving

**Qiang Li**

*Department of Civil Engineering, Zhejiang Ocean University, China  
Email: qiangli\_001@hotmail.com*

**Zhiqing Zhang**

*Urban Planning College, Zhejiang Shuren University, China  
Email: zhangzhiqing2000@163.com*

## ABSTRACT

It is well known that the surrounding soil is compacted during pile installation and the compaction region has an important effect on pile dynamic responses. In the present paper, the compaction zone is divided into two stages, namely the stage of soil compaction by pile driving and the one of pore pressure dissipation. At the stage of soil compaction, the excess pore pressure is built up in the compaction zone, after then the excess pore pressure dissipates gradually, it is so-called stage of pore pressure dissipation. Based on analysis of the two stages, a simplified model of pile vertical vibration which can reflect the soil compaction and dissipation of excess pore pressure is established considering the heterogeneous radial zone of soil in the vicinity of the pile disturbed by pile driving. An analytical solution is deduced in frequency domain by means of variable separating method and then a semi-analytical solution is obtained using numerical convolution method. Numerical results from the frequency domain indicate that the equivalent radius of compaction zone has major effect on pile dynamic response, as well as the ratio of exceed pore pressure. It can also be concluded that the actual interaction of pile and soil will be weakened due to the radial zone caused by pile driving, a fact can be deduced that the interaction of pile and soil is overestimated under the ideal undisturbed model. Pile dynamic test of compaction pile should be carried out as soon as possible in order to obtain greater depth of pile test.

**KEYWORDS:** interaction of soil and pile, pile driving, dynamic response, saturated soil, exceed pore pressure, soil/pile set-up

## INTRODUCTION

When pile is driving into saturated soil, the surrounding soil is compacted and exceed pore pressure is built up. After that, the exceed pore pressure dissipates gradually, accordingly, the strength of soil close to pile recovers<sup>1</sup>. Such a phenomenon called “thixotropy” has an impact on pile driving and bearing capacity of pile. It is well known that after installation, pile capacity

often increases with time and it is known as soil/pile set-up or time effects of pile driving<sup>2-4</sup>. Pile set-up is significant to develop for load and resistance factor design (LRFD) of driven piles<sup>5</sup>. National code limits the resting time for pile bearing capacity test, mainly taking the set-up into account. The pile set-up is dominated by the dissipation of excess pore pressure and the increase of pile side shear which has been widely explored both experimentally and theoretically<sup>6-8</sup>. The results of some researches show that the mechanisms for set-up of displacement piles can also be contributed to creep of soil<sup>9</sup>. However, few researches have concerned about the influence of thixotropy on pile dynamic response. Novak et al.<sup>10</sup> made a thin-layer-element method to study the pile vibration with a disturbance region surrounding the pile. Veletsos et al.<sup>11</sup> analyzed the vertical and torsion vibration of inhomogeneous foundation based on Novak's method. Yang et al.<sup>12</sup> studied the vertical dynamic response of pile considering the soil inhomogeneity in the radial direction by using annular model. Han et al.<sup>13</sup> successfully resolved boundary reflections for soil regions by a model with a continuous variation of shear modulus in the radial direction of disturbed area. In order to reveal the mechanism of pile vibration in saturated soil, several researchers studied the dynamic response of pile on the basis of poroelasticity. Zeng et al.<sup>14</sup> analyzed the vertical dynamic load transfer of an elastic bar in the saturated porous medium by virtue of boundary integral equations. Nogami et al.<sup>15</sup> established a contact element model of zero thickness, by means of recursive method to analysis the effect of exceed pore water pressure in poroelastic medium on pile vertical vibration. Li et al.<sup>16,17</sup> studied vertical vibration of pile in saturated soil under the assumption of imperfect contact on the surface of soil and pile and a homogenous soften regions with a constant modulus surrounded the pile using separation of variables method. But for the vertical vibration of pile in heterogeneous saturated porous medium induced by pile driving, there is no technical literature as we know.

In the present paper, a simplified dynamic interaction of soil and pile is established to analyze the vertical dynamic response of pile in the heterogeneous compaction regions of soil by pile installation. The soil compaction zone is divided into two stages, namely the stage of soil compaction and the one of pore pressure dissipation. At the stage of soil compaction, the excess pore pressure is built up in the compaction zone, after pile installation, the excess pore pressure dissipated gradually; it is so-called stage of dissipation. Based on analysis of the two different stages, a simplified model of pile vertical vibration which can reflect the soil compaction and dissipation of excess pore pressure is established considering the inhomogeneous radial zone of soil in the vicinity of the pile disturbed by pile driving. Such a model of soil and pile interaction is valuable for practice.

## SIMPLIFIED MODEL OF PILE VIBRATION IN SATURATED SOIL

When a compaction pile is installed in a saturated soil layer by pile driving, a radial disturbed zone in neighborhood of the pile is aroused, and shear modulus of the region usually decreases with the disturbance of soil expansion and pile vibration. Hereafter, the soil around the pile is divided into two annular regions: the inner, the soften field with shear modulus  $\mu_1$  and the outer, elastic undisturbed region with initial shear modulus  $\mu$ . A sketch of soil and pile interaction is shown in fig.1, where  $r_s$  denotes the radius of soften region,  $H$  and  $r_0$  are the length and radius of pile respectively,  $P(t)$  is an arbitrary exciting force applied at the pile head,  $k_s$  and  $k_b$  denote the subgrade and pile toe reaction coefficients, respectively.

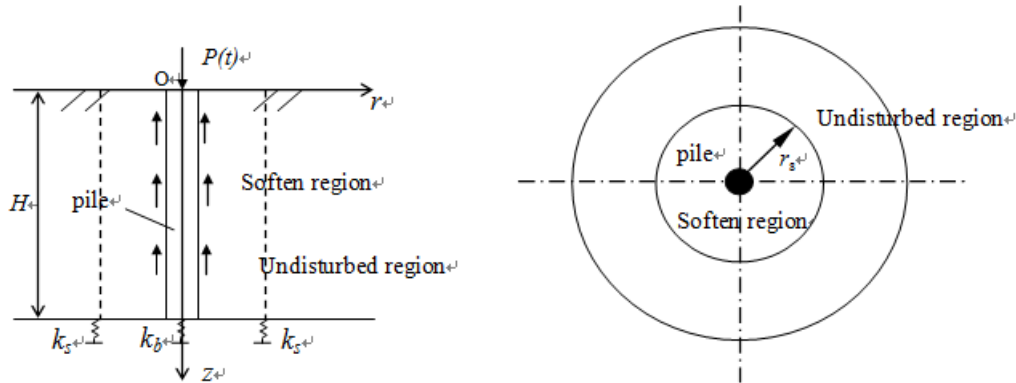


**Figure 1:** Sketch of soil-pile interaction

When the pile is driving, nonlinear behavior occurs in the soil region close to the pile. Few rigorous solutions can be used to model the interaction, so, a simplified model has to be established. In this paper, we study the compaction pile at two different stages, namely the compaction stage and the dissipation stage of exceed pore pressure.

At the stage of soil compaction, the radial total stress and the exceed pore pressure in the inner zone increases due to soil compaction caused by pile sinking, which can be expressed by means of cavity expansion theory. In this paper, we assumed that the total stress and exceed pore pressure of soften region satisfied the following equations respectively on the basis of some experimental results<sup>18,19</sup>.

$$\sigma = a_t - b_t \ln(\bar{r}) \tag{1}$$

$$\Delta u = a_p - b_p \ln(\bar{r}) \tag{2}$$

where  $a_t$  and  $a_p$  are known as the total stress and exceed pore pressure at pile shaft, respectively.

$b_t = (a_t - \sigma_0) / \ln \bar{r}_s$ ,  $b_p = a_p / \ln \bar{r}_s$ , in which  $\bar{r} = r/r_0$  is the equivalent radius of disturbed region.

At the stage of dissipation, the exceed pore pressure dissipates gradually, and accordingly, the soil strength recovers. Assumed that the total stress holds on and the excess pore pressure dissipates completely, we can conclude that the final effective stress is equal to the total stress. It can be expressed as

$$\sigma'_2 = \sigma = a_t - b_t \ln(\bar{r}) \tag{3}$$

At the two stages, dynamic responses of pile vertical vibration change with variations of soil properties surrounding the pile. Firstly, we study the variations of circumferential soil properties at the two stages.

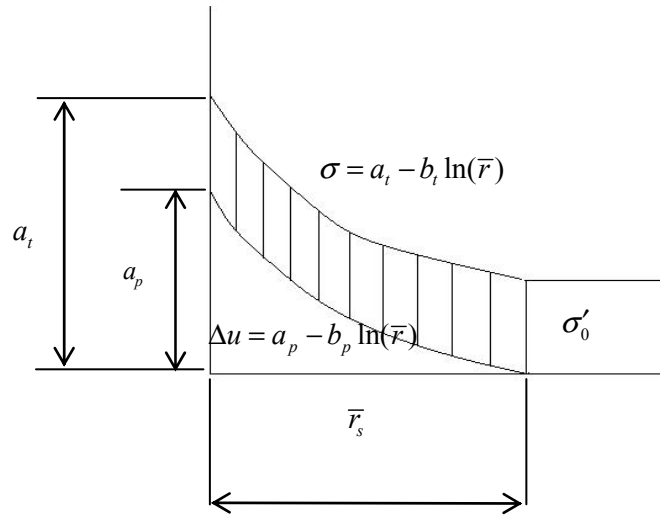


**Figure 2:** Sketch of stress and pore pressure of compaction

Stage I: Relative research indicates that the shear modulus of soil changes with the variation of effective stress due to the exceed pore pressure<sup>20</sup>. It can be expressed as

$$\mu_1(r)/\mu = \sqrt{\sigma'_1/\sigma'_0} \quad (4)$$

where  $\sigma'_0$  is the initial effective stress which is supposed as uniform distribution and  $\sigma'_1$  is the one after pile driving.

Substituting equation (1) and (2) into (3), we can obtain the following equation on a basis of effective stress principle.

$$\mu_1(r)/\mu = \sqrt{\sigma'_1/\sigma'_0} \Rightarrow \mu_1(r)/\mu = \sqrt{(\sigma - \Delta u)/\sigma'_0} = \sqrt{[(a_t - a_p) - (b_t - b_p) \ln \bar{r}]/\sigma'_0} \quad (5)$$

$$\beta' = \mu_1(r)/\mu = \sqrt{p_{r0} - (p_{r0} - 1) \ln \bar{r} / \ln \bar{r}_s} \quad (6)$$

where  $\beta'$  is ratio of shear stress,  $p_{r0} = (a_t - a_p)/\sigma'_0$  is known as ratio of effective stress at pile shaft. When  $1 > p_{r0} \geq 0$ , the ratio of shear stress gradually decreases with the distance  $r$ , so called “harden”, whereas  $p_{r0} \geq 1$ , it gradually increases and so called “soften”.

Thus, the ratio of shear modulus of the soil surrounding the pile before and after soil compaction is related to the distance from pile as well as affected by the equivalent radius of compaction zone and the ratio of effective stress at pile shaft due to soil compaction by pile installation.

Stage II: Similarly, at the stage of dissipation, the effective stress increases with the dissipation of exceed pore pressure, accordingly, the shear modulus increases gradually. Here, we neglect the course of dissipation of exceed pore pressure, and analyze the final state at which the exceed pore pressure dissipates completely.

$$\mu_2(r)/\mu = \sqrt{\sigma'_2/\sigma'_0} \Rightarrow \mu_2(r)/\mu = \sqrt{\sigma/\sigma'_0} = \sqrt{(a_t - b_t \ln \bar{r})/\sigma'_0} \quad (7)$$

$$\beta'' = \mu_2(r)/\mu = \sqrt{T_{r_0} - (T_{r_0} - 1) \ln \bar{r} / \ln \bar{r}_s} \quad (8)$$

where  $\beta''$  denotes the ratio of shear modulus at the stage II,  $T_{r_0} = a_t/\sigma'_0$  is called ratio of additional total stress at pile shaft. It should be especially paid attention to the range of  $T_{r_0}$ , namely  $T_{r_0} \geq 1$  and  $0 \leq T_{r_0} - P_{r_0} = a_p/\sigma'_0 \leq a_t/\sigma'_0 = T_{r_0}$  (It means that the exceed pore pressure can not exceed the total stress at pile shaft when soil surrounding the pile is compacted by pile installation, that is, no liquefaction will occur as well as the negative pore pressure).

Therefore, after the exceed pore pressure dissipates completely, the ratio of shear modulus of soil is related to the distance from pile as well as affected by the equivalent radius of soil compaction and additional total stress at pile shaft.

Based on the above analysis, we can find that the expression of ratio of shear modulus has the same form at the two stages. In the following analysis, we study the pile dynamic response with the first stage, and the solution of the second stage is common with the first one as well.

## ANALYSIS OF VIBRATION OF PILE AND SOIL

### Vibration of compaction region

Assumed that soften region is annular, the relationship of stress and strain of inner soil region is linear and neglecting the soil quality of soften region, the equation of vertical motion of the inner medium can be expressed under plane strain condition as

$$\frac{\partial(\bar{r}\bar{\tau}_{rz1})}{\partial\bar{r}} = 0 \quad (9)$$

$$\bar{\tau}_{rz1} = \beta'(1+iD) \frac{\partial\bar{u}_{z1}}{\partial\bar{r}} \quad (10)$$

where  $i = \sqrt{-1}$ ,  $\bar{\tau}_{rz1} = \tau_{rz1}/\mu$ ,  $\bar{u}_{z1} = u_{z1}/r_0$ ,  $\beta' = \mu_1/\mu$ ,  $\bar{r} = r/r_0$ ,  $\bar{r}_s = r_s/r_0$ ,  $D$  is the coefficient of hysteretic type damping, in which,  $\tau_{rz1}$ ,  $u_{z1}$  are the shear stress and vertical displacement of soften region, respectively.

The boundary conditions of soften region can be expressed as

$$\bar{u}_{z1}|_{\bar{r}=1} = \bar{w}_b \quad \bar{u}_{z1}|_{\bar{r}=\bar{r}_s} = \bar{u}_z|_{\bar{r}=\bar{r}_s} \quad \bar{\tau}_{rz1}|_{\bar{r}=\bar{r}_s} = \bar{\tau}_{rz}|_{\bar{r}=\bar{r}_s} \quad \bar{\tau}_{rz1}|_{\bar{r}=1} = -f/(2\pi r_0 \mu) \quad (11)$$

where  $\bar{w}_b = w_b/r_0$ ,  $\bar{u}_z = u_z/r_0$ ,  $\bar{\tau}_{rz} = \tau_{rz}/\mu$ ,  $w_b$  is the displacement of pile,  $\tau_{rz}$ ,  $u_z$  are the shear stress and vertical displacement of undisturbed region, respectively.  $f$  denotes the unit skin friction of pile.

From Eqs. (4), (5) and (6), we can deduce the solution of the shear stress.

$$\bar{\tau}_{rz1}|_{\bar{r}=1} = \frac{(1+iD)(1+\sqrt{p_{r0}})}{2 \ln \bar{r}_s} (\bar{u}_{z2}|_{\bar{r}=\bar{r}_s} - \bar{w}_b) \quad (12)$$

$$\bar{\tau}_{rz1}|_{\bar{r}=\bar{r}_s} = \frac{(1+iD)(1+\sqrt{p_{r0}})}{2\bar{r}_s \ln \bar{r}_s} (\bar{u}_{z2}|_{\bar{r}=\bar{r}_s} - \bar{w}_b) \quad (13)$$

### Undisturbed Region

The undisturbed areas are dealt with two-phase saturated soil theory originated by Biot<sup>21</sup>. For axisymmetric problem, the governing equations of motions of saturated soil can be expressed as

$$\mu \nabla^2 u + (\lambda_c + \mu) \nabla \nabla \cdot u + \alpha M \nabla \nabla \cdot w = \rho \ddot{u} + \rho_f \ddot{w} \quad (14)$$

$$\alpha M \nabla \nabla \cdot u + M \nabla \nabla \cdot w = \rho_f \ddot{u} + m \ddot{w} + b \dot{w} \quad (15)$$

where  $\nabla^2 = \frac{\partial^2}{\partial r^2} + \frac{1}{r} \frac{\partial}{\partial r} + \frac{\partial^2}{\partial z^2} = \frac{1}{r} \frac{\partial}{\partial r} (r \frac{\partial}{\partial r}) + \frac{\partial^2}{\partial z^2}$ ,  $u$  and  $w$  denote the average displacement vectors of solid matrix and fluid relative to solid matrix, respectively.  $\rho$  and  $\rho_f$  denote mass densities of the bulk material and the pore fluid respectively;  $\rho = (1-n)\rho_s + n\rho_f$ , where  $n$  is porosity of soil and  $\rho_s$  denotes mass density of grains.  $m = \rho_f/n$  denotes a density-like parameter that depends on  $\rho_f$  and the geometry of the pores;  $b = \rho_f g / k_B$  denotes a parameter accounting for the internal friction due to the relative motion between the solid matrix and the pore fluid, that is, so-called seepage force, where  $k_B$  denotes the coefficient of permeability of the medium and  $g$  denotes the gravity acceleration.  $\lambda_c = \lambda + \alpha^2 M$ , in which  $\lambda$  and  $\mu$  are Lamé's constants.  $\alpha$  and  $M$  denote the Biot's parameters accounting for compressibility in the two-phase material and can be determined by  $\alpha = 1 - K_b/K_s$ ,  $M = K_s^2/(K_d - K_b)$ ,  $K_d = K_s[1 + n(K_s/K_f - 1)]$ , in which  $K_s$ ,  $K_f$  and  $K_b$  are the bulk modulus of solid grains, fluid and soil skeleton, respectively.

The boundary conditions of the saturated soil layer are:

(1) Stresses and displacements approach zero at an infinite horizontal distance;

(2) Zero normal stresses on the free surface  $\sigma_z(r, 0) = 0$

(3) The soil layer bears on an elastic base,  $E_s \pi r_0^2 \frac{\partial u_z}{\partial z}(r, H) + k_s u_z(r, H) = 0$

(4) Impervious on contact surface of disturbed and undisturbed zone due to smear effect,  $w_r(r_s, z) = 0$

(5) Zero radial displacement on pile shaft,  $u_r(r_s, z) = 0$

Using variable separation method, the governing differential equations of the undisturbed region of saturated soil are decoupled by introducing the potential functions, by means of the boundary conditions, the shear stress and vertical motion of soil can be obtained as

$$\bar{\tau}_{zr}|_{\bar{r}=\bar{r}_s} = \sum_{n=1}^{\infty} \eta'_{1n} C_{1n} \cosh(h_n z) \quad (16)$$

$$\bar{u}_z|_{\bar{r}=\bar{r}_s} = \sum_{n=1}^{\infty} \eta'_{2n} C_{1n} \cosh(h_n z) \quad (17)$$

where  $\eta'_{1n} = 2(1 + \frac{h_{1n}^2}{h_n^2}) \frac{\lambda_1 - \lambda_2}{\lambda_2 - \lambda_5} g_{1n} h_n K_1(g_{1n} \bar{r}_s)$ ,

$$\eta'_{2n} = 2h_n K_0(g_{1n} \bar{r}_s) - \frac{2(\lambda_1 - \lambda_5) g_{1n} h_n K_1(g_{1n} \bar{r}_s) K_0(g_{2n} \bar{r}_s)}{(\lambda_2 - \lambda_5) g_{2n} K_1(g_{2n} \bar{r}_s)} - \frac{2(\lambda_1 - \lambda_2) g_{1n} h_n K_1(g_{1n} \bar{r}_s) K_0(h_{1n} \bar{r}_s)}{(\lambda_2 - \lambda_5) h_n K_1(h_{1n} \bar{r}_s)}$$

The coefficient  $h_n$  satisfies the transcendental equation:  $h_n \sinh(h_n \theta) + k_s^* \cosh(h_n \theta) = 0$ , in

which  $\theta = H/r_0$  stands for the slenderness ratio of pile,  $k_s^* = k_s r_0 / E_s$  denotes the dimensionless

coefficient of subgrade reaction.  $g_{1n}^2 + h_n^2 = \beta_1^2$ ,  $g_{2n}^2 + h_n^2 = \beta_2^2$ ,  $h_{1n}^2 + h_n^2 = \gamma^2$ .  $I_0(gr)$ ,  $K_0(gr)$

are the first category zero-order imaginary variation Bessel function and the second one,

respectively.  $\lambda_c^* = \lambda^* + \alpha^2 M^* = \lambda/\mu + \alpha^2 M/\mu$ ,  $\rho^* = \rho_f/\rho$ ,  $\delta = \sqrt{\rho/\mu} s r_0$ ,  $m^* = m/\rho$ ,

$$b^* = b r_0 / \sqrt{\rho \mu} \quad , \quad D_f = c_f / k_f \quad , \quad \beta_{1,2}^2 = \frac{d_1 \pm \sqrt{d_1^2 - 4d_2}}{2} \quad , \quad \gamma^2 = \frac{-\rho^{*2} \delta^4 + (m^* \delta^2 + b^* \delta) \delta^2}{m^* \delta^2 + b^* \delta} \quad ,$$

$$d_1 = \frac{(\lambda_c^* + 2)(m^* \delta^2 + b^* \delta) + M^* \delta^2 - 2\alpha \rho^* M^* \delta^2}{(\lambda^* + 2)M^*} \quad , \quad d_2 = \frac{(m^* - \rho^{*2}) \delta^4 + b^* \delta^3}{(\lambda^* + 2)M^*} \quad ,$$

$$\lambda_i = \frac{-\alpha M^* \beta_i^2 + \rho^* \delta^2}{M^* \beta_i^2 - (m^* \delta^2 + b^* \delta)} \quad , \quad i = 1, 2 \quad , \quad \lambda_5 = -\frac{\rho^* \delta^2}{m^* \delta^2 + b^* \delta} \quad .$$

## Dynamic Response of Pile

The motion of pile with initial static state can be expressed as

$$\frac{d^2 \bar{w}_b}{dz^2} - \frac{\rho_b^* \delta^2}{E_b^*} \bar{w}_b = -\frac{2}{E_b^*} \bar{\tau}_{zr1}|_{\bar{r}=1} \quad (18)$$

$$\left( \frac{d\bar{w}_b}{d\bar{z}} + k_b^* \bar{w}_b \right) \Big|_{\bar{z}=\theta} = 0 \quad , \quad \frac{d\bar{w}_b}{d\bar{z}} \Big|_{\bar{z}=\theta} = \bar{P}^*(s) \quad (19)$$

where  $E_b^* = E_b/\mu$ 、 $\rho_b^* = \rho_b/\rho$ 、 $k_b^* = k_b/(E_b\pi r_0)$ 、 $\bar{P}^* = \bar{P}/(\mu\pi r_0^2)$ 、in which  $E_b$  and  $\rho_b$  denote the elastic modulus and density of pile, respectively.

The perfect contact condition is satisfied on the contact surface of pile and soil.

$$\bar{u}_{z1}(r_0, z) = \bar{w}_b(z) \quad (20)$$

Based on the continuous conditions of the contact surface in the pile and soil, also in the disturbed and undisturbed regions, the dynamic response of the coupled system can be solved according to the orthogonal property of hyperbolic cosine function.

$$\bar{w}_b = A_1 e^{\kappa z} + B_1 e^{-\kappa z} + \sum_{n=1}^{\infty} \frac{-(1+iD)(1+\sqrt{p_{r0}})\eta'_{2n} C_{1n}}{E_b^*(h_n^2 - \kappa^2) \ln \bar{r}_s} \cosh(h_n z) \quad (21)$$

where  $G_n = h_n \sinh(h_n \theta) + k_b^* \cosh(h_n \theta)$ 、 $\kappa^2 = \frac{\rho_b^* \delta^2}{E_b^*} + \frac{(1+iD)(1+\sqrt{p_{r0}})}{E_b^* \ln \bar{r}_s}$ 、 $C_{1n} = A_1 E_n + B_1 F_n$ 、

$$A_1 = \frac{\frac{\bar{P}^*}{E_b^* \kappa} [(k_b^* - \kappa) e^{-\kappa \theta} + \sum_{n=1}^{\infty} \frac{-(1+iD)(1+\sqrt{p_{r0}})\eta'_{2n} F_n G_n}{E_b^*(h_n^2 - \kappa^2) \ln \bar{r}_s}]}{(k_b^* + \kappa) e^{\kappa \theta} + (k_b^* - \kappa) e^{-\kappa \theta} + \sum_{n=1}^{\infty} \frac{-(1+iD)(1+\sqrt{p_{r0}})\eta'_{2n} (E_n + F_n) G_n}{E_b^*(h_n^2 - \kappa^2) \ln \bar{r}_s}}$$

$$B_1 = -\frac{\frac{\bar{P}^*}{E_b^* \kappa} [(k_b^* + \kappa) e^{\kappa \theta} + \sum_{n=1}^{\infty} \frac{-(1+iD)(1+\sqrt{p_{r0}})\eta'_{2n} E_n G_n}{E_b^*(h_n^2 - \kappa^2) \ln \bar{r}_s}]}{(k_b^* + \kappa) e^{\kappa \theta} + (k_b^* - \kappa) e^{-\kappa \theta} + \sum_{n=1}^{\infty} \frac{-(1+iD)(1+\sqrt{p_{r0}})\eta'_{2n} (E_n + F_n) G_n}{E_b^*(h_n^2 - \kappa^2) \ln \bar{r}_s}}$$

$$E_n = \frac{\frac{e^{(\kappa+h_n)\theta} - 1}{2(\kappa+h_n)} + \frac{e^{(\kappa-h_n)\theta} - 1}{2(\kappa-h_n)}}{[\eta'_{2n} + \frac{(1+iD)(1+\sqrt{p_{r0}})\eta'_{2n}}{E_b^*(h_n^2 - \kappa^2) \ln \bar{r}_s} - \frac{2\bar{r}_s \ln \bar{r}_s \cdot \eta'_{1n}}{(1+iD)(1+\sqrt{p_{r0}})}] [\frac{\theta}{2} + \frac{\sinh(2h_n \theta)}{4h_n}]}$$

$$F_n = -\frac{\frac{e^{-(\kappa-h_n)\theta} - 1}{2(\kappa-h_n)} + \frac{e^{-(\kappa+h_n)\theta} - 1}{2(\kappa+h_n)}}{[\eta'_{2n} + \frac{(1+iD)(1+\sqrt{p_{r0}})\eta'_{2n}}{E_b^*(h_n^2 - \kappa^2) \ln \bar{r}_s} - \frac{2\bar{r}_s \ln \bar{r}_s \cdot \eta'_{1n}}{(1+iD)(1+\sqrt{p_{r0}})}] [\frac{\theta}{2} + \frac{\sinh(2h_n \theta)}{4h_n}]}$$

Assumed that  $s = i\omega$ 、the complex stiffness of pile-soil system at pile head can be expressed as

$$k_d = \frac{1}{A_1 [1 + \sum_{n=1}^{\infty} \frac{-(1+iD)(1+\sqrt{p_{r0}})\eta'_{2n} E_n}{E_b^*(h_n^2 - \kappa^2) \ln \bar{r}_s}] + B_1 [1 + \sum_{n=1}^{\infty} \frac{-(1+iD)(1+\sqrt{p_{r0}})\eta'_{2n} F_n}{E_b^*(h_n^2 - \kappa^2) \ln \bar{r}_s}] } \quad (22)$$

The admittance of pile at the pile head is

$$|H_v(i\omega)| = |1/k_d| \quad (23)$$

When a transient force such as a half-sine pulse imposed on the pile head, the response of velocities at the pile head can be developed by inverse Fourier transform and convolution.

$$V(t) = IFT \left[ H_v(i\omega) \cdot P_{\max} \omega \frac{1 + e^{-\pi s/\omega}}{\omega^2 + s^2} \right] \quad (24)$$

Similarly, the solutions of the second stage are consistent with the first stage, just substituting  $T_{r0}$  for  $P_{r0}$ .

## NUMERICAL ANALYSIS

In this section, numerical results are calculated based on the above solutions. Unless otherwise specified, the following parameter values are used:  $\lambda^* = 9.00$ ,  $M^* = 57.75$ ,  $\rho^* = 0.52$ ,  $m^* = 1.15$ ,  $\alpha = 0.98$ ,  $b^* = 1337.50$ ,  $E_b^* = 500$ ,  $\rho_b^* = 1.29$ ,  $\theta = 40$ ,  $k_b^* = 1.0$ ,  $k_s^* = 1.0$ ,  $\bar{r}_s = \sqrt{2}$ ,  $D = 0.02$ .

### Comparison of Perfect Contact Undisturbed Model and Compaction Pile Model

For compaction pile, when  $T_{r0} = 1$  and  $\bar{r}_s \rightarrow 1$ , or  $P_{r0} = 1$  and  $\bar{r}_s \rightarrow 1$ , the pile is approximate non-soil compaction pile, which should be coincident with the analytical solutions of pile vertical vibration in saturated soil on the basis of perfect contact undisturbed model given in reference<sup>22</sup>. Hereafter, we compare the pile complex stiffness and admittance amplitude in frequency domain of the present paper with the ones shown in above mentioned reference. The comparisons of the two pile vibration models are shown in figure 3, where X-axis is the dimensionless frequency  $\bar{f} = 2\pi r_0 f / \omega_g$ , in which  $f$  is the frequency of pile and  $\omega_g$  is the natural frequency of pile to satisfy  $\omega_g / c = k_b^* \cot(\omega_g \theta / c)$  simultaneously,  $c$  is the compressive wave velocity of pile. For the sake of convenience, the dynamic stiffness has been normalized by the static stiffness at  $\omega = 0$  as shown in figure 3. From figure 3, we can see that the complex stiffness and the pile admittance in the present solutions are in good agreement with those in the perfect contact undisturbed model. It implies that the present model can degenerate to the perfect contact undisturbed model under above mentioned conditions.

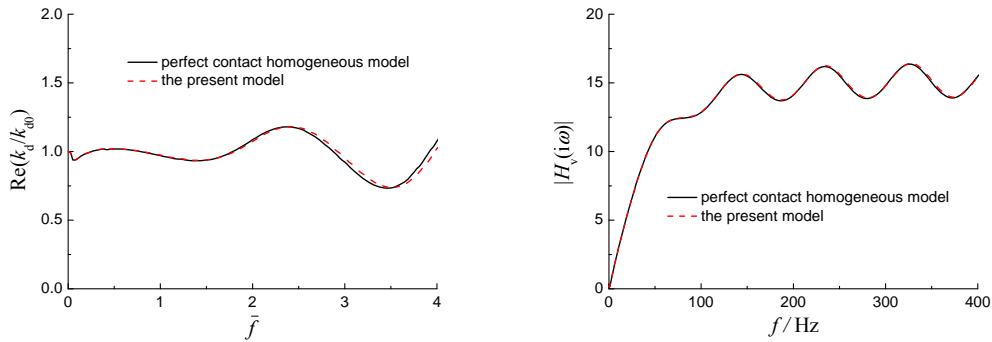


**Figure 3:** Comparison of pile dynamic response for two models

### Effects of the properties of Compaction zone on the Pile Dynamic Response

Based on the analysis in section 2, vertical vibration of compaction pile is divided into two stages. Hereafter, we study the effects of properties of two stages on the pile dynamic response.

#### Analysis of Stage I

The effects of soil properties of compaction region at the stage I, namely the ratio of effective stress at pile shaft  $p_{r0}$ , the equivalent radius of soften region  $\bar{r}_s$  and hysteretic coefficient  $D$ , on the admittance and complex stiffness in the frequency domain are illustrated from Fig. 4 to 6.

#### (1) Effect of $p_{r0}$ on pile dynamic response

From figure 4, we find that the amplitude of pile admittance and the stiffness at pile head decreases with the increasing ratio of effective stress, which can be due to binding of soil to pile increases with the increasing ratio of effective stress.

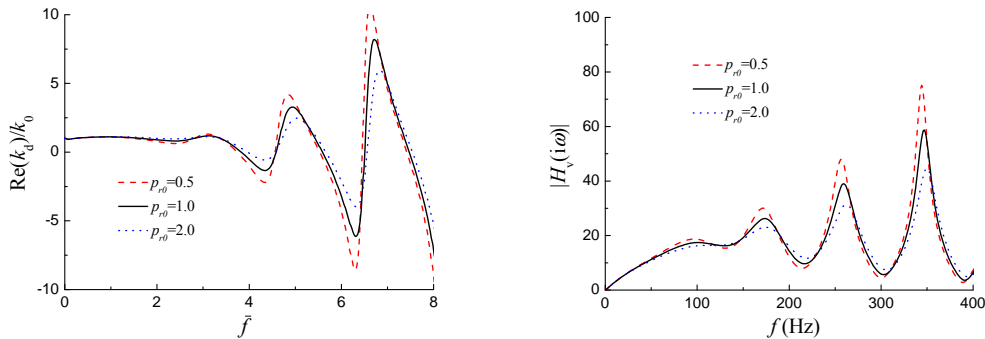
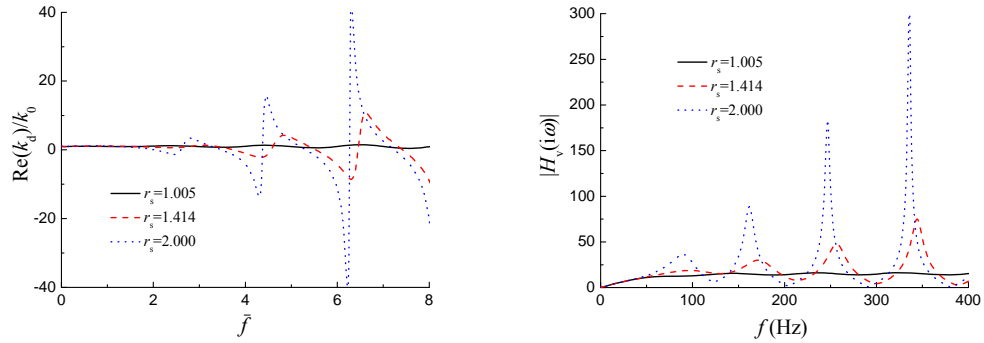
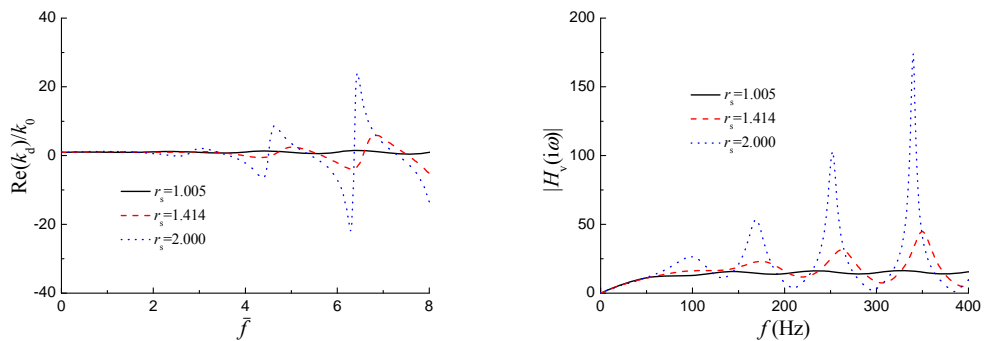


**Figure 4:** Effects of  $p_{r0}$  on pile admittance and reflection



(1) Soften



(2) Harden

**Figure 5:** Effects of radiuses of soften zone on pile dynamic responses

(2) Effect of  $\bar{r}_s$  on pile dynamic response

From Figure 5 we can see that there are significant effects of the equivalent radius of compaction zone on the pile dynamic response. Whether the soften or the harden, the dynamic stiffness and admittance of pile are rapid increased with the increasing equivalent radius, which can be explain that the larger equivalent radius of soil compaction zone is, the stronger effect of compaction is, furthermore, the weaker effect of the binding of soil to pile, thus the larger amplitude of vibration.

(3) Effect of hysteretic damping on pile dynamic response

Figure 6 shows that the amplitude of stiffness and admittance at pile head increase with the increasing hysteretic damping, however, the influence is minor to the above two parameters.

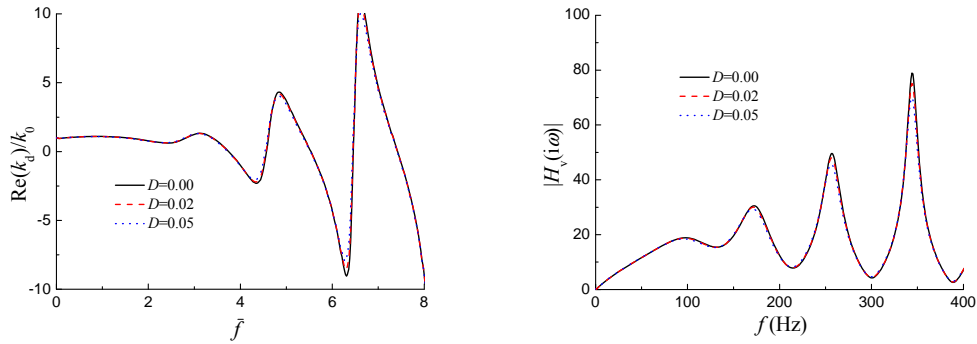


**Figure 6:** Effects of hysteretic damping on pile dynamic responses

### Analysis of Stage II

At the stage II, we study the effects of the ratio of additional total stress  $T_{r0}$  on the pile dynamic responses. In order to compare with the stage I, a two-stage method which contains two kinds of comparisons is applied to analysis dynamic response of pile. One is the same ratio of effective stress, but the ratio of additional total stress is different from the other, another is vice versa.

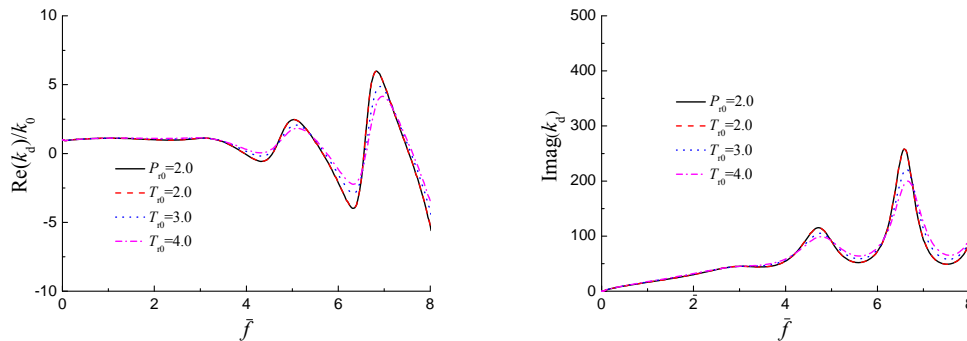


**Figure 7:** Effects of hysteretic damping on pile admittance and reflection

Figure 7 shows the comparisons of complex stiffness before and after dissipation of exceed pore pressure under different ratios of additional total stress. For the harden compaction pile, when  $T_{r0} = P_{r0}$ , the complex stiffness in the two cases is similar because pore pressure does not build up. When the ratio of total stress increases, the deviation of complex stiffness is increasing apparent. The amplitude of complex stiffness decreases with the increasing ratio of additional total stress. This implies that the larger of the ratio of total stress is, the stronger the bonding of soil to pile when the consolidation is completed is for a certain ratio of effective stress.

Figure 8 shows the comparisons of complex stiffness after exceed pore pressure dissipates under different ratios of effective stress at a certain ratio of total stress. It can be seen from figure 8, the amplitude of dynamic stiffness and damping after dissipation of exceed pore pressure decrease with the increasing ratio of effective stress. This implies that the bonding of soil to pile increases with the increasing ratio of effective stress.

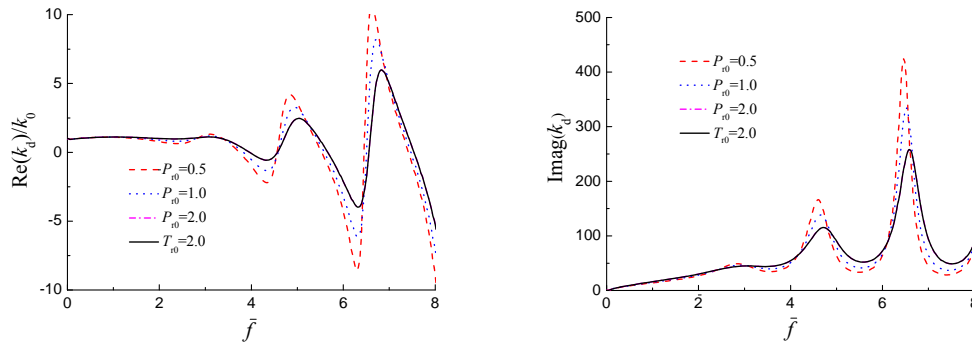


**Figure 8:** Effects of hysteretic damping on pile admittance and reflection

## DISCUSSION OF APPLICATION

A two-stage analysis of vertical vibration of compaction pile has an important guiding significance for the engineering practice. In this section, a time-domain reflectometry analysis is performed for engineering application, as shown in Figure 9. Figure 9(1) shows the comparison of time-domain reflectometry at several different equivalent radiuses of soil compaction zone with the perfect contact homogeneous model. Figure 9(1) shows the larger equivalent radius of soil compaction zone is, the stronger time-domain reflectometry is. Figure 9(1) also shows that equivalent radius of soil compaction zone (such as  $\bar{r}_s = 1.005$ ) is minimal, and corresponding to non displacement pile, the time-domain reflectometry is coincidence with the perfect contact homogeneous model. Figure 9(2) gives time-domain reflectometry at the two stages under different effective stress ratio on the conditions of soil compaction and dissipation of pore pressure. From Figure 9(2), it can be seen that the smaller effective stress ratio is, the stronger the reflection at pile head is. When the effective stress ratio and the additional total stress ratio are equal ( $P_{r0} = T_{r0}$ ), and so is the time domain reflection of pile. The greater difference of effective stress ratio and the additional total stress, the greater difference in the peak is. But relatively, the effect of the effective stress or the total stress is smaller than the equivalent radius of soil compaction. Actually, time effect of displacement pile is more obvious than the semi-

displacement or non-displacement pile. After pile sinking, because of the existence of thixotropic restoration, the exceed pore pressure gradually dissipates, and the soil strength gradually recovers, furthermore the peak of time domain reflection decreases. Therefore, in order to obtain a clear reflection at the pile head, the test should be done as soon as possible, so that the greater test depth can be obtained. This is different from the static load test of pile to wait until the soil strength is somewhat recovered.

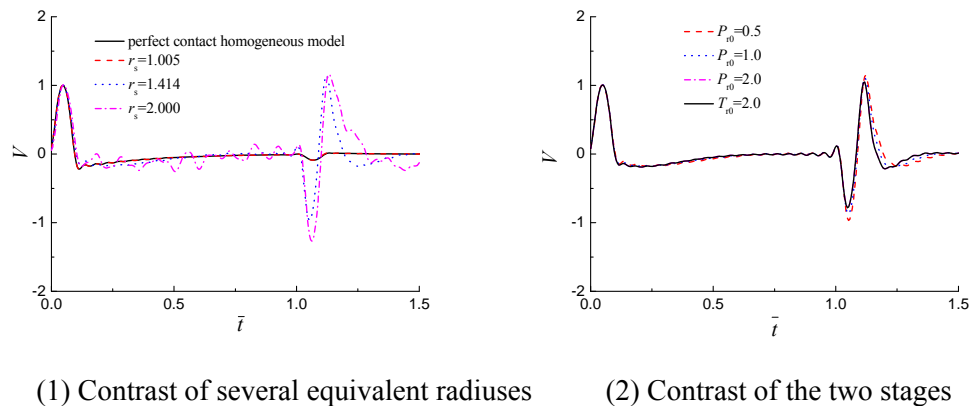


**Figure 9:** Effects of slenderness of pile on reflection wave curves

## CONCLUSIONS

- (1) A simplified model is established to consider the compaction region caused by pile sinking, analytical solutions are derived by means of variable separation method. Numerical results show that the present solution can be degenerated to the perfect contact homogeneous model.
- (2) Numerical results show that the equivalent radius of compaction region has obvious effects on the characteristics of vertical vibration of pile and the effect of hysteretic damping is minor.
- (3) The present model can reflect the effects of soil set-up to a certain extent and it also can be used in the pile low strain test.
- (4) Taking the complexity of such a problem into account, the current solution still is worth discussing in many aspects, such as large strain problems of soil compaction, strain accumulation under the action of vibration, change of soil mass structure during thixotropic restoration, and so on, these problems need further study, but this solution can be served as a useful attempt.

## ACKNOWLEDGEMENTS

This work is supported by: National Natural Science Foundation of China under Grant No. 50879077 and Priority subject project of Science and Technology Hall of Zhejiang Province under Grant No. 2007C13065, Science and Technology Program of Transport Hall of Zhejiang Province under Grant No. 2009H21.

## REFERENCES

1. Randolph, M.F., Carter, J.P., and Wroth, C.P. (1979). "Driven Piles in Clay – the Effects of Installation and Subsequent Consolidation." *Géotechnique* 29(4), 361-393.
2. Ng, W.K., Selamat, M.R. and Choong, K.K. (2010) "Soil/Pile Set-up Effects on Driven Pile in Malaysian Soil." *EJGE*, 2010, 15(Bund. A), 1-11.
3. Titi, H.H., and Wathugala, G.W. (1999) "Numerical Procedure for Predicting Pile Capacity –Setup/Freeze". *Transportation Research Record* 1663, Paper No.99-0942, 25-32.
4. Komurka, V.E., Wagner, A.B., and Edil, T.B. (2003) "Estimating Soil/Pile Set-up". Wisconsin Department of Transportation, USA WHRP Report No. 03-05.
5. Yang, L. and Liang, R. (2009). "Incorporating setup into load and resistance factor design of driven piles in sand". *Can. Geotech. J.* 46, 296–305.
6. Guo, W.D. (2000). "Visco-elastic consolidation subsequent to pile installation". *Computers and Geotechnics*, 26, 113-144.
7. Bullock, P.J., Schmertmann, J.H., McVay, M.C. et al. (2005). "Side Shear Setup. I: Test Piles Driven in Florida". *Journal of Geotechnical and Geoenvironmental Engineering*, 131(3), 292–300.
8. Bullock, P.J., Schmertmann, J.H., McVay, M.C. et al. (2005). "Side Shear Setup. II: Results From Florida Test Piles". *Journal of Geotechnical and Geoenvironmental Engineering*, 131(3), 301–310.
9. Bowman, E.T. and Soga, K. (2005) "Mechanisms of setup of displacement piles in sand: laboratory creep tests". *Can. Geotech. J.* 42, 1391–1407.
10. Novak, M., Nogami T. and Aboul-Ella F. (1978) "Dynamic soil reactions for plane strain case". *J. Engineering Mechanics*, 104(EM4), 953-959.
11. Veletsos, A.S. and Dotson, K.W. (1986) "Impedance of soil layer with disturbed boundary zone". *J Geotechnical Engineering*. 112(3), 363-368.
12. Yang, D.Y., Wang, K.h., Zhang, Z.Q., Leo, C.J. (2008) "Vertical dynamic response of pile in a radially heterogeneous soil layer". *International Journal for Numerical and Analytical Methods in Geomechanics*. 33(8), 1039-1054.
13. Han, Y.C. and Sabin, G.C.W. (1995) "Impedance for radially inhomogeneous viscoelastic soil media". *Journal of Engineering Mechanics*., 121(9), 939-947.
14. Nogami, T., Ren, F.Z. and Chen J.W. (1997) "Vertical vibration of pile in vibration-induced excess pore pressure field". *J. Geotechnical and Geoenvironmental Engineering*, 123(5), 422-429.
15. Zeng, X. and Rajapakse, R.K.N.D. (1999) "Dynamic axial load transfer from elastic bar to poroelastic medium". *J. Engineering. Mechanics*, 125(9), 1048-1055.
16. Li Q. (2007) "Vertical vibration of piles embedded in saturated soil considering the imperfect contact". *Journal of Hydraulic Engineering*, 38(3), 349-354(in Chinese).

17. Li, Q., Sun, Z.J. and Gao, H.X. (2008) "Vertical Vibration of Pile in Saturated Soil Considering Soften Regions of Surrounding Soil". Proceedings of the 14th World Conference on Earthquake Engineering, Beijing, China.(in CD-ROM)
18. Carter, J.P., Randolph, M.F. and Wroth, C.P. (1979) "Stress and pore pressure changes in clay during and after the expansion of a cylindrical cavity". International J. Numerical and Analytical Methods in Geomechanics. 3, 305-322.
19. Lee, F. H. Juneja, A. and Tan T.S. (2004) "Stress and pore pressure changes due to sand compaction pile installation in soft clay". Geotechnique, 54(1), 1-16.
20. Martin, P.P. and Seed, H.B. (1979) "Simplified procedure for effective stress analysis of ground response". J. Geotechnical Engineering, 105(GT6), 739-758.
21. Biot, M.A., (1956) "Theory of propagation of elastic waves in a fluid-saturated porous solid □. low-frequency range". J. Acoustic. Society America, 28(2), 168-178.
22. Wang G.M., Li, Q., Wang, K.H. (2006), "Simplified Model for Vertical Vibration of Pile in Single-layer Saturated Soil and its Analytical Solution". Chinese Journal of Rock Mechanics and Engineering, 25(z2): 4233-4241. (in Chinese)

